RESEARCH ARTICLE

# Purification and concentration of infectious koi herpesvirus using steric exclusion chromatography

Friederike Eilts[1] | Lisa K. Jordan[2] | Yasmina M. J. Harsy[1] | Sven M. Bergmann[3,4,5] | Anna M. Becker[2] | Michael W. Wolff[1]

[1]Institute of Bioprocess Engineering and Pharmaceutical Technology, University of Applied Sciences Mittelhessen, Giessen, Germany

[2]Institute of Bioprocess Engineering, Friedrich-Alexander University Erlangen-Nürnberg, Erlangen, Germany

[3]Friedrich-Loeffler-Institute, Federal Research Institute for Animal Health, Institute of Infectiology, Greifswald - Insel Riems, Germany

[4]Jockey Club College of Veterinary Medicine and Life Sciences, City of Hong Kong, Kowloon, Hong Kong

[5]Avicare+, Köthen, Germany

**Correspondence**
Sven M. Bergmann, Friedrich-Loeffler-Institute, Federal Research Institute for Animal Health, Institute of Infectiology, Greifswald - Insel Riems, Germany.
Email: saint_michel@gmx.de

Michael W. Wolff, Institute of Bioprocess Engineering and Pharmaceutical Technology, University of Applied Sciences Mittelhessen, Giessen, Germany.
Email: michael.wolff@lse.thm.de

## Abstract

Koi herpesvirus (KHV) is the causative agent of a koi herpesvirus disease (KHVD) inducing high mortality rates in common carp and koi (*Cyprinus carpio*). No widespread effective vaccination strategy has been implemented yet, which is partly due to side effects of the immunized fish. In this study, we present an evaluation of the purification of infectious KHV from host cell protein and DNA, using the steric exclusion chromatography. The method is related to conventional polyethylene glycol (PEG) precipitation implemented in a chromatographic set-up and has been applied for infectious virus particle purification with high recoveries and impurity removal. Here, we achieved a yield of up to 55% of infectious KHV by using 12% PEG (molecular weight of 6 kDa) at pH 7.0. The recoveries were higher when using chromatographic cellulose membranes with 3–5 μm pores in diameter instead of 1 μm. The losses were assumed to originate from dense KHV precipitates retained on the membranes. Additionally, the use of >0.6 M NaCl was shown to inactivate infectious KHV. In summary, we propose a first step towards a purification procedure for infectious KHV with a possible implementation in fish vaccine manufacturing.

**KEYWORDS**
cyprinid herpesvirus 3, downstream processing, fish health management, fish vaccination, vaccine manufacturing

## 1 | INTRODUCTION

KHV, also known as *Cyprinid herpesvirus 3*, is a large and complex ds DNA virus (170–230 nm; Hedrick et al., 2005). It is the causative agent, like all herpesviruses do, of a latent infection (Eide et al., 2011) in cyprinids, the KHVD, with a morbidity and mortality of up to 100% (Bergmann et al., 2010; Haenen et al., 2004). Considering the high mortality rate and the rapid spreading of the KHV, an outbreak causes disastrous damage for natural habitats and for aquacultures. Despite great efforts and the development of various vaccines against this reportable finfish disease in recent years (Adamek et al., 2022; Hu et al., 2021; Liu et al., 2018, 2020; Ma et al., 2020), no effective virus candidates against KHVD are licenced apart from KV3 in Israel (Bergmann et al., 2020; Dishon et al., 2014). Among the

reasons for this development are the need for attenuated KHV vaccine candidates (Adamek et al., 2022) and adverse reactions caused by adjuvants or host cell-induced impurities (Sommerset et al., 2005; Vandenberg, 2004). Such side effects can be circumvented by using an advanced purification procedure. For KHV, up to now, only small-scale strategies for analytical purification of infectious virus, for example by centrifugation (Bergmann et al., 2017), and DNA concentration from freshwater samples, for example using cation binding filtration (see Supplementary Material), have been applied.

In contrast to human vaccines, levels of residual impurities for veterinary vaccines are insufficiently regulated by health authorities. The European Medicinal Agency, for example, advises that the bioburden should be held as low as possible (EMA/CVMP/IWP/206555/2010-Rev.1). Thus, little has been published about purification strategies for fish vaccines. Another challenge for the fish vaccine production is a low cost–benefit-ratio (Sommerset et al., 2005; Yanong & Erlacher-Reid, 2012). Often, lesser than 10 cents per fish for a full immunization are reported for vaccination of aquatic living animals.

A possible purification method that meets the stated requirements is the steric exclusion chromatography (SXC). It is an economic, quick and easy-to-use method, which enabled high yields (>80%–90%) for previously published applications of (infectious) viral particles (Alvim et al., 2021; Eilts, Lothert, Orbay et al., 2022, Eilts, Steger, Pagallies et al., 2022; Gränicher et al., 2021; Labisch et al., 2022; Lee et al., 2012; Lothert, Offersgaard, Pihl et al., 2020, Lothert, Pagallies, Eilts et al. 2020, Lothert, Sprick, Beyer et al., 2020; Marichal-Gallardo et al., 2017, 2021). The impurity removal reaches 80%–100% for protein and >60% for host cell DNA without any enzymatic DNA digestion steps. The employed materials are polyethylene glycol (PEG), a buffering system for formulation and a hydrophilic stationary phase, for example cellulose membranes (Figure 1b1–3). The SXC relies, just as conventional PEG precipitation, on the mutual crowding-out of molecules. In more detail, the formation of a PEG-deficient zone around the virions induces their precipitation. In contrast to conventional precipitation, the stationary phase is part of the precipitation system. Hence, it is covered by a PEG-deficient zone, that is sterically excluded by the PEG, as well (Figure 1b3). Thus, the virions not only attach among each other but also to the stationary phase to increase the thermodynamical stability of the system. In other words, the virions precipitate on the stationary phase, which allows for a chromatographic bind-and-elute mode. The process is governed by several factors: (1) By increasing the size and concentration of the solutes, that is PEG and virus particles, the steric exclusion effect is increased as the thickness of the PEG-deficient zone is increased. Therefore, bigger molecules are excluded with lower PEG concentrations and vice versa. (2) The surface characteristics of the virions, for example the charge, regulate their attraction and repulsion. A reduced repulsion and, thus, an increased virus precipitation, can be achieved by, for example charge shielding with an increased ionic strength of the applied solution, or by adapting the pH to reduce the surface charge. (3) The nature of the stationary phase, including

hydrophilicity and pore size, determines the binding of the precipitates, which is the working principle of SXC. It should be pointed out here that the virions precipitate on the stationary phase, which contrasts with conventional PEG precipitation, where already existing precipitates are filtered from the solution. Filtration is a limitation to SXC, as it causes pore clogging and high-pressure surges (Figure 1c; Eilts, Lothert, Orbay et al., 2022). For further details, we recommend publications on the foundations of SXC (Gagnon et al., 2014; Lee et al., 2012).

In this work, SXC was screened as a purification method for KHV from virus-infected cell culture supernatants. Process parameters of interest were the PEG concentration and molecular weight, the pH, the pore size of the stationary phase and the ionic strength. With this report, we hope to support the development of effective vaccines against KHV and other fish diseases, by proposing an economic method to purify KHV for vaccination, which might increase the safety and efficacy of future vaccine candidates.

## 2 | MATERIALS AND METHODS

### 2.1 | Generation of virus stock

The Taiwanese KHV isolate KHV-T was propagated in common carp brain cells (CCB) (Wang et al., 2015). Both, virus and cells, were obtained by the courtesy of the Friedrich-Loeffler-Institute. Cell cultivation and virus inoculation were performed using DMEM (Sigma-Aldrich) supplemented with 10% foetal bovine serum (Sigma-Aldrich) at 25°C, if not stated otherwise. Virus stocks were either prepared using T75 flasks (Sarstedt), as described by Amtmann et al. (2020), with a total volume of 20 mL DMEM per flask, or in siliconized spinner flasks (glassware, Integra Bioscience) using CCB cells immobilized on Cytodex 3 microcarriers (GE Healthcare). For the latter, 3 mg mL$^{-1}$ of sterilized carriers, together with $3.5 \times 10^5$ cells mL$^{-1}$, were seeded in 200 mL of media and incubated for 9 days, while being stirred at 75 rpm and 25°C. For virus inoculation, the carriers were left for sedimentation, and 70 mL of supernatant were discarded, before $4 \times 10^6$ KHV particles (determined via virus titration and expressed as 50% tissue culture infective dose, TCID$_{50}$) were added. The suspension was stirred for 60 min, and thereafter, the volume was adjusted with fresh DMEM to 200 mL. Three days post-infection, the supernatant was harvested. The collected virus suspension was frozen at −80°C. The titres of generated virus stocks ranged from $10^7$ to $10^9$ TCID$_{50}$ mL$^{-1}$. The clarification, that is removal of cell debris, of the KHV stocks was conducted by thawing the cell culture supernatant, followed by consecutive centrifugation (250×$g$ for 10 min, 4500×$g$ for 30 min and 15,000×$g$ for 10 min). Afterwards, the virus suspension was frozen again at −80°C until further use. The KHV was not inactivated or attenuated in any kind, to enable the validation of the KHV infectivity. For all studies, the KHV samples were stored on ice and protected from light.
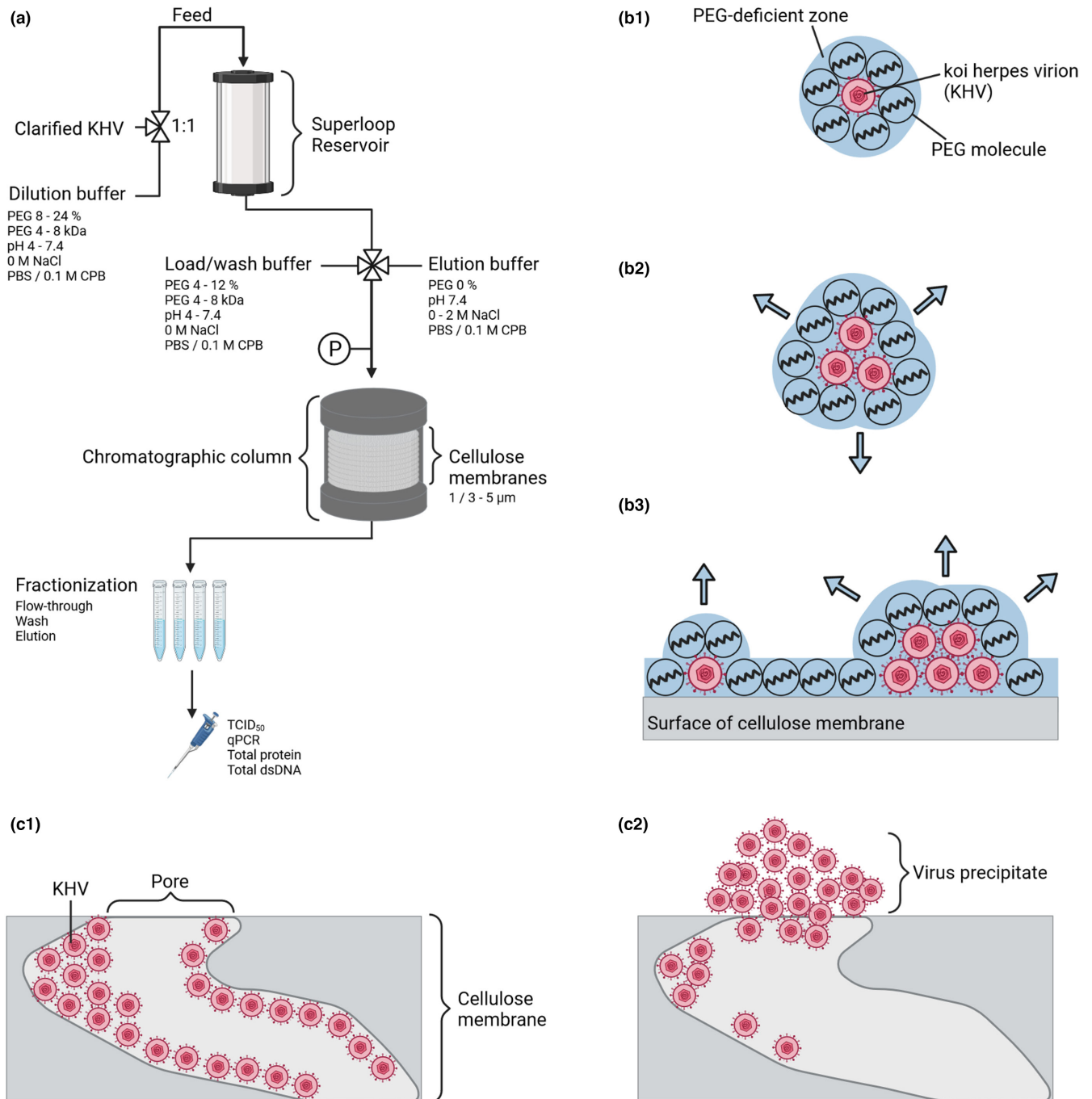
**FIGURE 1** Working principle of SXC experiments. (a) Schematic representation of chromatographic set-up with an ÄKTA system. A sample of clarified KHV is combined with a PEG solution (dilution buffer), generating the feed, and loaded into a 10 mL superloop. The feed is loaded onto the chromatographic column, consisting of a stack cellulose membranes. Afterwards, the column is washed (wash buffer) and the sample eluted (elution buffer). All samples are fractionated, and the fractions analysed. (b1-b3) The principle of SXC is based on crowding-out effects. (b1) The KHV particles are surrounded by PEG molecules, which cannot fill the adjacent full space. Thus, a so-called PEG-deficient zone forms. (b2) By adhering towards each other, that is precipitating, the interface and the volume of the PEG-deficient zone are reduced, which releases water into the surrounding PEG-rich bulk solution. This process is thermodynamically favourable. (b3) In SXC, the stationary phase is part of the precipitation system, and covered by a PEG-deficient zone. Thus, KHV binds at the surface of cellulose membranes, and is retained throughout loading. (c1) Ideally, the inner surface of the porous cellulose membranes is consecutively covered with the retained KHV particles, and loading is limited either by a sample breakthrough at the maximal loading capacity, or by a pressure increase due to a full coverage of the pores. (c2) However, if precipitation is too rapid, big KHV precipitates can block the pores without binding at the inner surface. This causes filtration effects and pressure surges, which eventually reduce the column capacity. The figure was prepared using biorender.com.

## 2.2 | KHV quantification

### 2.2.1 | TCID$_{50}$ assay

Infective KHV particles in samples were analysed using the TCID$_{50}$ assay, as described previously (Jordan et al., 2017). Briefly, CCB cells in 100 μL DMEM were seeded into 96-well plates (Greiner bio-one) with a cell density of 40,000 cells cm$^{-2}$ and incubated overnight for cell attachment at 25°C. The next day, the virus-containing samples were thawed and a 10-fold dilution series up to 10$^{-8}$ was prepared using DMEM. Afterwards, the supernatant of the cell culture was discarded, and 100 μL of each dilution was added to the cells in eight wells at a time. The inoculated cells were incubated and, after 10–14 days, checked for cytopathic effects (CPE) using bright-field microscopy. A statistical analysis was performed according to Reed and Muench (1938). The samples from the SXC were diluted 1:10 to reduce possible interferences of NaCl and PEG with the assay (Supplementary Material S1.1).

### 2.2.2 | qPCR

The concentration of KHV DNA, corresponding to the concentration of the virus particles, was assessed via DNA extraction (Jordan et al., 2017) and subsequent qPCR, according to Gilad et al. (2004) with minor modifications. Briefly, the DNA was extracted using the DNeasy Blood and Tissue Kit (Qiagen). For this procedure, the samples were diluted 1:10 with nuclease-free water according to an evaluation of the influence of PEG and NaCl on the assay (Supplementary Material S1.2). Afterwards, the qPCR was prepared with the QuantiTect Probe PCR Kit (Qiagen). Here, 5 μL of the extracted DNA was added to 20 μL master mix, comprising nuclease-free water, 2×reaction mix, primers and probe (Sigma-Aldrich; final concentration 1 μM). The TaqMan PCR amplification was done in a Mastercycler ep gradient S realplex$^2$ (Eppendorf) or a CFX Connect Real Time System (Bio-Rad) with the following programme: (1) 5 min at 95°C, (2) followed by 40 cycles of 15 s at 95°C and (3) one cycle of 60 s at 60°C. A standard with a previously determined number of copy numbers was used to quantify the KHV DNA.

## 2.3 | Characterization of the KHV

### 2.3.1 | Osmotic stability evaluation

At first, the stability of infective KHV particles, in relation to the osmotic pressure, was assessed. For this purpose, a virus stock was prepared in DMEM containing 10% foetal bovine serum. This stock was diluted 1:2 with PBS supplemented with various NaCl concentrations, to adjust to total NaCl (Carl Roth) concentrations, ranging from 0.1 M NaCl (control) to 2.1 M. Afterwards, the samples were incubated at 4°C for 2 h. Next, the concentration of infective virus particles was analysed via virus titration. Afterwards, the same samples

were transferred to −80°C for 8 days, and the concentration of infectious virus particles was measured again.

### 2.3.2 | Isoelectric point determination

SXC-purified virus particles were analysed for their isoelectric point, as described previously, with minor modifications (Eilts, Steger, Pagallies et al., 2022). In brief, purified KHV, stored in PBS (Gibco), was diluted 1:5 with 0.1 M citrate (VWR Chemicals) phosphate (Carl Roth) buffer (CPB) (adjusted to 15 mS cm$^{-1}$ with NaCl), or in PBS with 0.03% (v/v) polysorbate 20 (Carl Roth), both at pH values ranging from 3 to 11. The pH of the CPB was titrated with citrate- or Na$_2$PO$_4$-stock solutions, and the pH of PBS with HCl (Carl Roth). Measurements of the electrophoretic mobility, and thus zeta potential, were performed in triplicates directly after sample preparation in folded capillary zeta cells (#DTS1070, Malvern Panalytical), using a Zetasizer Nano ZS90 (Zetasizer 7.13 software, Malvern Panalytical).

### 2.3.3 | Precipitation behaviour in dependence of PEG concentration and pH

Time-dependent size measurements of the KHV-containing cell culture supernatant were conducted via dynamic light scattering, adapted from Eilts, Lothert, Orbay et al. (2022). Therefore, clarified virus suspension was mixed in equal parts with CPB (15 mS cm$^{-1}$) of a defined pH (4–7.4) and PEG-6000-concentration (Carl Roth) (0%–12%). The analysis was conducted in micro-cuvettes (Sarstedt) using a Zetasizer Nano ZS90, which allowed for automatic measurements every 5 min over the course of 60 min. Afterwards, the samples were examined for visible aggregates by bright-field microscopy in conventional Neubauer chambers, which were used to analyse at a constant volume. To generate a model of the pH- and PEG-dependent aggregate sizes, a design of experiments (DOE)-based approach (Design Expert 12 software, Stat-Ease) was applied (Supplementary Material S4.1).

## 2.4 | SXC purification procedure

Prior to all chromatographic procedures, the cell culture-derived KHV was clarified by consecutive centrifugation, as described above. The SXC runs were performed either on an Äkta Prime Plus or an Äkta Pure 25 (Cytiva) according to a standard procedure (Lothert et al., 2021), described here in short. Each single-use column consisted of 10 membrane discs of regenerated cellulose with a nominal pore size of either 1 μm (GE Healthcare Life Sciences) or 3–5 μm (kindly provided by Sartorius Stedim). Three different buffers were prepared for each SXC run: (1) The equilibration buffer consisted of either PBS or 0.1 M CPB (adjusted to 15 mS cm$^{-1}$) with a defined pH between 4 and 7.4. The buffers were supplemented with PEG of different sizes (4–8 kDa) and concentrations (4%–12%). (2) The sample preparation buffer was composed in the same way

as the respective equilibration buffer, but with twice the concentration of the corresponding PEG. Last, (3) the elution buffer corresponded to the respective buffering system that was used for the previous two buffers, but was of a neutral pH (pH 7.4) and without PEG. Additionally, up to 2 M NaCl was added to the elution buffer in some cases. An overview of the SXC set-up is visualized in Figure 1a.

For every SXC run, the membrane stacks were equilibrated with the equilibration buffer, and next, the KHV suspension was loaded onto the columns. For this purpose, the virus suspension was mixed with the sample preparation buffer (1:2) and instantly filled into a superloop. After sample loading, the membranes were washed with the equilibration buffer (2–4 mL), and the virus subsequently eluted using the elution buffer with half of the loading volume, but with at least 4 mL. The flow rate for all runs was 2 mL min$^{-1}$, and the loading volume was defined by the maximum precolumn pressure limit (1 MPa). All samples were frozen at −80°C until further use. The recoveries of infectious KHV, virus DNA and the residual impurity content in the individual runs were assessed on a volumetric basis, related to the respective feed concentrations.

## 2.5 | Statistical evaluation of critical process parameters of the SXC for the recovery of infectious KHV

Two distinct DOE-based approaches were used for the identification of critical process parameters for the purification of KHV using SXC (Design Expert 12 software). First, three factors were varied: the (1) PEG concentration (4%–10%), (2) the PEG molecular weight (4–8 kDa) for the virus loading onto the column and (3) the NaCl concentration (0%–2%) for the elution of KHV from the column (Supplementary Material S3.1 and Table S3). In a second design, only the PEG concentration (4%–10%) and the PEG molecular weight (4–8 kDa) in the loading buffer were varied without an addition of NaCl to the elution buffer (Supplementary Material S3.2 and Table S5). All buffers were prepared using PBS at pH 7.4, and the chromatographic material consisted of cellulose membranes with 1 μm pore size. Loading was performed with 10 mL of KHV with $5 \times 10^6$ TCID$_{50}$ mL$^{-1}$ [$3 \times 10^9$ viral DNA copy number (cn) mL$^{-1}$], or until the pressure limit was reached. All fractions from the SXC runs were characterized with regard to the viral DNA concentration, but only the feed and the elution were assessed for their infectious KHV contents. Using these data, the losses of infectious KHV and viral DNA in the elution were modelled.

## 2.6 | Analysis of impurities

Chromatographic fractions, that is feed, flow-through, wash and elution, were analysed with regard to the levels of protein and DNA, as previously described (Lothert, Pagallies, Feger et al., 2020). For the total protein assay, all samples were diluted at least 1:2, according to a study on the influence of PEG and NaCl on the assay (Supplementary Material S1.3).

## 3 | RESULTS

## 3.1 | Definition and optimisation of critical SXC process parameters for the purification of infectious KHV

So far, no studies have explored the purification, capture or concentration of herpesviruses via SXC. Thus, in the first DOE-based model (Supplementary Material S3.1 and Table S3), we explored three critical process parameters for the application of SXC to purify infectious KHV, based on previous virus studies (Lothert, Sprick, Beyer et al., 2020; Supplementary Material S3.1 and Table S4): (1) the PEG concentration (4%–10%) and (2) the PEG molecular weight (4–8 kDa) in the loading buffer, as well as (3) the NaCl concentration in the elution buffer (0–2 M). The study aimed to identify the loss of infectivity and viral DNA content, which was calculated according to the volumetric yield of KHV DNA and infectious KHV in the elution fraction in comparison with their initial content in the feed, which was loaded onto the column (100%).

Concerning the loss of infectious KHV throughout the SXC application, the NaCl concentration (factor C) and the interaction of NaCl and the PEG concentration (factor BC) were significant. In detail, the loss of infectious KHV ranged from 1.1 to 7.0 log TCID$_{50}$ mL$^{-1}$ of the initial $5 \times 10^5$–$1 \times 10^7$ TCID$_{50}$ mL$^{-1}$. The loss of infectious viral particles increased with higher NaCl concentrations (factor C) (Figure 2a–c). For the lowest PEG molecular weight (4 kDa), an increasing PEG concentration elevated this effect (Figure 2a), and vice versa for the highest PEG molecular weight (8 kDa) (Figure 2c). Hence, a higher PEG molecular weight was beneficial for infectious KHV recovery. The highest infectious KHV yield, that is the lowest losses, was achieved with 10% PEG-6000 or PEG-8000 in the loading buffer without NaCl in the elution buffer. Next, the viral DNA loss ranged from 60% to 90% compared with the initial KHV DNA content of approximately $6 \times 10^8$ cn mL$^{-1}$ (Figure 2d–f). The losses were influenced significantly by the PEG molecular weight (factor A$^2$), the PEG (factor B) and the NaCl concentrations (factor C), as well as their interactions (factor BC). The overall lowest KHV DNA loss in the elution fraction was predicted with 57% for high PEG-6000 or PEG-8000 concentrations (10%) in the loading buffer and low NaCl concentrations (0 M) in the elution buffer. Thus, for both responses, KHV DNA and infectious KHV particles were the highest for high PEG concentrations (10% PEG-6000 or PEG-8000) in the loading buffer and without a NaCl addition in the elution buffer.

In a second DOE-based experimental plan (Supplementary Material S3.2 and Table S5), KHV processing with SXC was further characterized without an addition of NaCl to the elution buffer. All other parameters were the same as in the set-up described before (Supplementary Material S3.2 and Table S6). The model showed that the predominant factor for both responses, the loss of infectious KHV and the loss of viral DNA, was the PEG concentration, whereas the PEG molecular weight was of no significance. An increasing PEG concentration reduced the KHV DNA losses in the elution fraction. These results supported the optimal process conditions found in
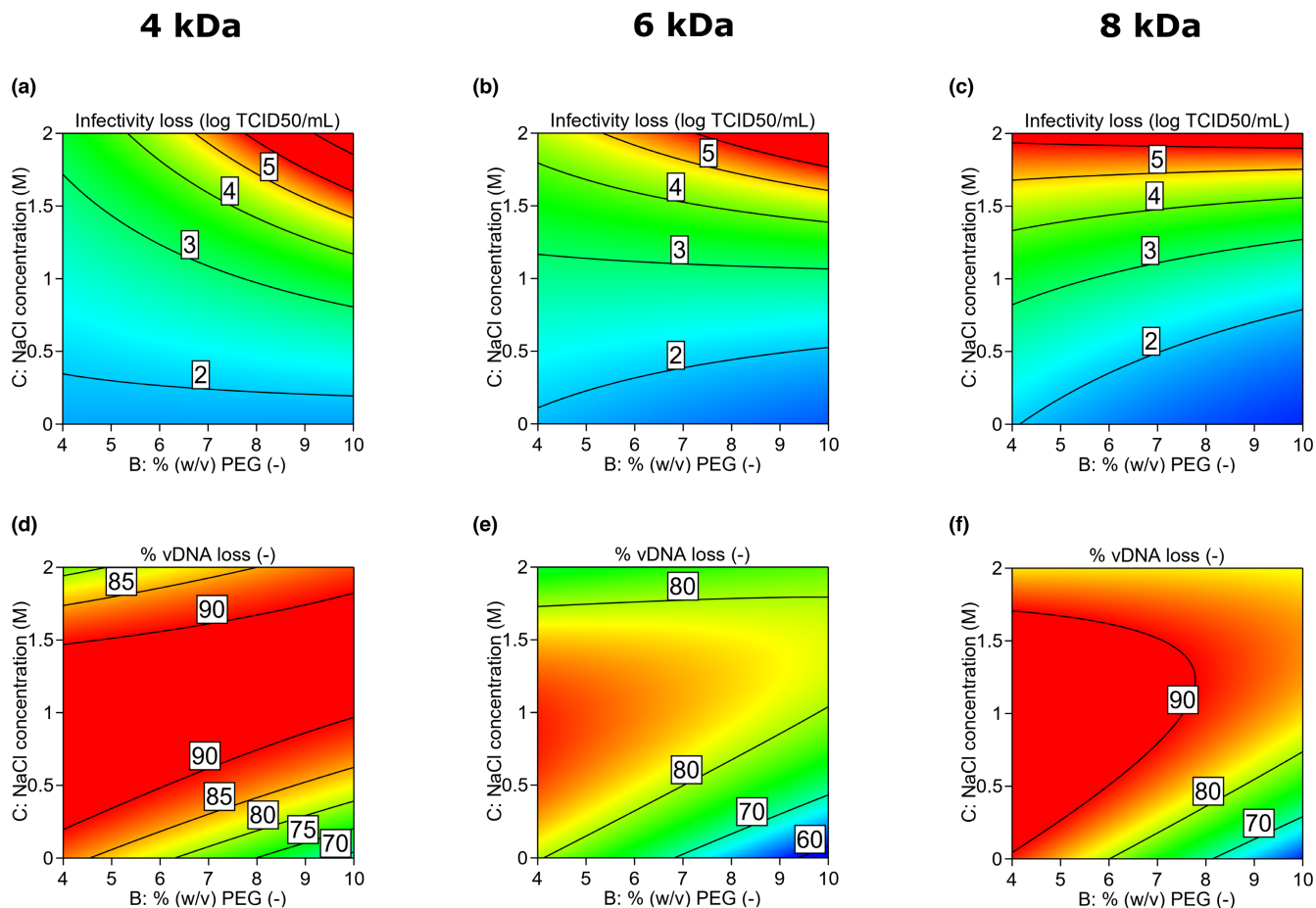
## 4 kDa   6 kDa   8 kDa



**FIGURE 2** Statistical evaluation of virus loss in SXC. KHV was processed via SXC under varying molecular weights (factor A) and concentrations (factor B) of PEG in the loading buffer. Additionally, the elution buffer was supplemented with NaCl (factor C). The losses of infectious viruses in the elution fraction were determined via titration as $\log TCID_{50}\ mL^{-1}$ (a–c), compared with the concentration in the feed. Accordingly, the relative loss of viral DNA (vDNA) (d–f) referred to the initial concentration in the feed fraction. The data were statistically analysed using a design of experiments-based software, generating models for each response (Table S6). The colouring of the contour plots was coded as follows: for loss of infectivity (a–c) 5–6 $\log TCID_{50}\ mL^{-1}$ (red), 4–5 $\log TCID_{50}\ mL^{-1}$ (yellow), 3–4 $\log TCID_{50}\ mL^{-1}$ (green) and 0–2 $\log TCID_{50}\ mL^{-1}$ (blue); concerning the vDNA loss (d–f), 85%–95% (red), 80%–85% (yellow), 70%–80% (green) and 60%–70% (blue).

the previous DOE model. Minimum losses of infectivity with 1.2 log $TCID_{50}\ mL^{-1}$ were predicted for the use of 10% PEG-8000 (Figure 3a). The same parameters were optimal for minimal viral DNA losses (65%) (Figure 3b). Additionally, the SXC runs performed with optimal conditions, that is 10% PEG-8000, exhibited $34 \pm 5\%$ and $12 \pm 3\%$ of the initial KHV DNA in the flow-through and wash fractions, respectively (data not shown). Accordingly, the total recoveries of the KHV DNA, of all fractions combined, reached $69 \pm 14\%$.

### 3.2 | Influence of different pore sizes of the stationary phase

By using 10% PEG-6000 for SXC loading, the viscosity-induced backpressure in the liquid chromatography system increased significantly. In this context, the impact of the pore size of the regenerated cellulose stationary phase, either 1 or 3–5 μm, was evaluated. Exemplary chromatograms of the operation with the two different

column types are depicted in Figure 4. Both columns were loaded with a 10% PEG-6000/KHV solution ($1–2 \times 10^7\ TCID_{50}\ mL^{-1}$) until the pressure maximum (1.5 MPa) of the liquid chromatography system was reached. The pressure increase showed an exponential pattern for the 1 μm membranes, while it remained near-linear for the 3–5 μm set. Thus, the bigger pore sizes, 3–5 μm, allowed for an increase in the loading volume by 20%, that is 8 mL compared with 10 mL for 1 and 3–5 μm, respectively. Using an elution volume of 4 mL, the initial KHV load was concentrated 1.25 times (considering the two-fold dilution with the concentrated PEG solution to generate the feed for column loading). Throughout loading, the dynamic light scattering signal, representing viral particles, revealed the breakthrough of unbound KHV for both membrane types. Concerning the 1 μm membranes, a constant particle breakthrough of 10% of the maximum dynamic light scattering signal was observed, while the 3–5 μm membranes showed a high initial signal, which rapidly decreased to 500 units, and then gradually decreased to 250 units throughout sample loading. The unbound virus particles observed
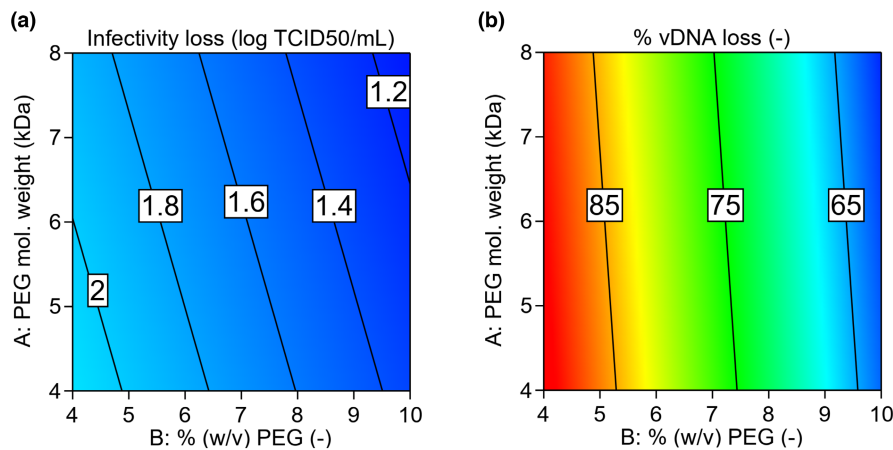
**FIGURE 3** KHV loss in a SXC application without NaCl addition. The SXC was operated with varying PEG concentrations and molecular weights. Each elution fraction was analysed with regard to the loss of infectious KHV by the $TCID_{50}$ assay (a), and vDNA by qPCR (b), compared with the respective content in the feed. The statistical analysis of the data was performed with a design of experiments-based software, generating models for each response (Table S8). The contour plot colouring represents (a) 0–2 log $TCID_{50}$ $mL^{-1}$ in blue for the infectivity loss, and concerning the virus DNA loss (b), 85%–95% (red), 80%–85% (yellow), 70%–80% (green) and 60%–70% (blue).
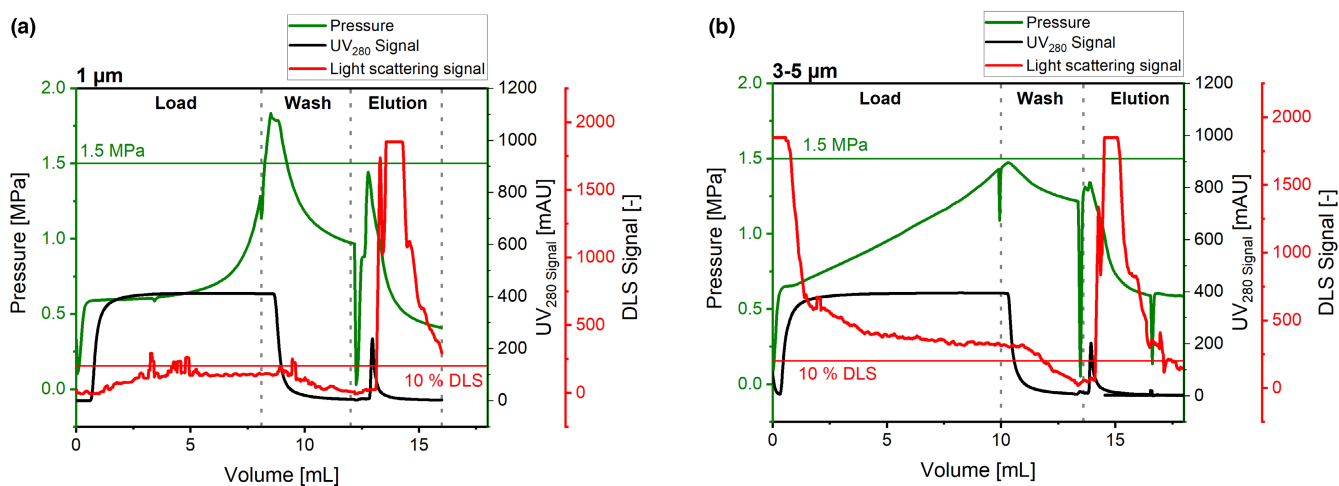


**FIGURE 4** Operating the SXC with chromatographic membranes of different pore sizes. KHV was purified by SXC with two different sets of regenerated cellulose membranes as stationary phases. Both columns consisted of regenerated cellulose membranes with either 1 μm (a) or 3–5 μm (b) in nominal pore diameter. Apart from the membranes, both runs were operated with the same conditions, that is 10% PEG-6000 in the loading buffer at a neutral pH. The online monitoring included the precolumn pressure (green), the $UV_{280}$ signal (black) and dynamic light scattering (DLS) signal (red). Each run was structured into the phases: load, wash (4 mL) and elution phase (4 mL). The maximum loading volume was determined by the pressure, and the sample application was stopped at 1.5 MPa (green reference line) as a precaution to prevent an overshooting of the maximum for the chromatographic system of 2 MPa.

by DLS in the loading fraction corresponded to a loss of KHV DNA of more than 40% for both membrane types (data not shown).

In the next step, to evaluate whether the KHV breakthrough throughout loading and consequently the KHV yield in the elution fraction can be improved, the PEG-6000 concentration was increased. A PEG-6000 concentration of 12%, sample loading onto the 1 μm cellulose columns was prevented by a pressure surge. The load volume for the 3–5 μm membranes was reduced to 4 mL, as compared to 10 mL with 10% PEG-6000 (Figure 5a, pH 7.4). For the application of 12% PEG-6000, more than 20% KHV DNA was found in the elution fraction. However, only 25±8% of KHV DNA was

recovered from the cellulose membranes in total, including flow-through, wash and elution fraction (Figure 5b, pH 7.4).

## 3.3 | Detecting residual KHV on cellulose membranes after SXC

As described in sections 3.1 and 3.2, the KHV DNA was not fully recovered in the combined chromatographic fractions. Thus, the 3–5 μm chromatographic membranes were stained with an anti-KHV dot blot after the SXC application (Supplementary Material S2). The
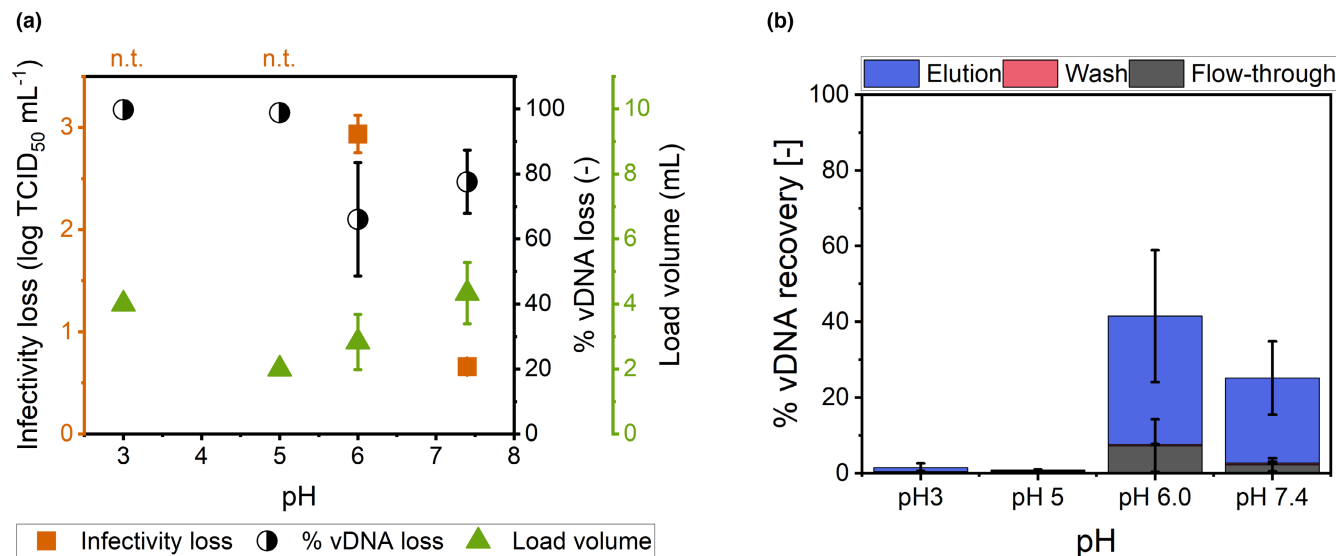
**(a)**



**(b)**



**FIGURE 5** SXC of KHV with varying pH. KHV was purified via SXC with varying pH values of the loading buffer. The cellulose membranes had a nominal pore diameter of 3–5 μm. Each run was performed with 12% PEG-6000 in citrate phosphate buffers of pH values of 3.0, 5.0, 6.0 or 7.4. For the elution, the pH was adjusted to a neutral pH, and the PEG concentration was reduced to 0%. (a) For each run, the infectious KHV (orange squares) and the vDNA (black, half-filled circles) loss in the elution fraction were assessed. The loss of KHV infectivity in the elution fraction was expressed as a logarithmic $TCID_{50}$ decrease in the initial concentration in the feed, while pH 3.0 and 5.0 were not tested (n.t.) due to virus inactivation (Amtmann et al., 2020). The loss of vDNA in the elution was normalized to the initial loading concentration (100%). Last, the respective maximum loading volume (green triangles) of the KHV-PEG solution at each pH is depicted. (b) The chromatography fractions flow-through (grey), wash (pink) and elution (blue) were collected and analysed concerning the vDNA concentration. In this case, the vDNA recoveries (not the losses) were normalized to the initial loading concentrations (100%). This data in part represent the results from (a), but they are shown again for comparative reasons. Runs at pH 6.0 and 7.4 were performed in triplicates, however, at pH 3.0 and 5.0 in duplicates.

SXC experiments were performed as described in the previous section, using a 12% PEG-6000/KHV mixture (pH 7.4). Immunoblotting of the upper five membranes showed a visible staining of the membranes processed with KHV and both antibodies as well as with KHV and conjugate, (Figure S5). Each first (upmost) membrane exhibited a strong signal, which was reduced on the following membranes.

## 3.4 | Variation of the pH value to optimize the KHV yield

The application of the cellulose membranes with a 3–5 μm pore diameter was further characterized with 12% PEG-6000 at pH values 3, 5, 6 and 7.4 in CPB, with the elution at a neutral pH. Figure 5a presents the KHV DNA concentration for all four conditions as a loss of KHV DNA with the lowest value (66 ± 17%) achieved for pH 6.0, followed by pH 7.4 (78 ± 10%). However, both applications reached a total viral DNA recovery of less than 45% (Figure 5b). Considering the concentration of KHV in the eluate, pH 7.4 performed better than the other pH values with nearly $4 \times 10^9$ cn mL$^{-1}$ (Table 1). By lowering the pH value, the loss of KHV DNA reached ≥99% in the elution fraction, and <2% were recovered totally. The loading capacity of the 3–5 μm membranes under optimal process conditions was $1.7 \pm 0.7 \times 10^9$ cn per square cm of the membrane (cm$^2_{membrane}$)$^{-1}$. In these experiments, the total membrane surface was 13.3 cm$^2$.

**TABLE 1** KHV and impurity concentrations in the eluate.

| | | pH 6 | pH 7.4 |
|---|---|---|---|
| Infectious KHV | $TCID_{50}$ mL$^{-1}$ | $2.15 \pm 1.8 \times 10^5$ | $5.62 \pm 0.7 \times 10^5$ |
| KHV DNA | cn mL$^{-1}$ | $1.5 \pm 0.1 \times 10^9$ | $3.9 \pm 2.6 \times 10^9$ |
| dsDNA | ng mL$^{-1}$ | $2.8 \pm 1.9$ | $7.5 \pm 6.1$ |
| Protein | μg mL$^{-1}$ | 57.0[a] | 53.5[a] |

*Note*: SXC runs were performed with 3–5 μm membranes. KHV was loaded onto the column as a 12% PEG-6000 solution at either pH 6 or 7.4, and eluted at pH 7.4 without a NaCl addition.

[a]No standard deviation was determined, as the protein content was below the limit of detection of the BCA assay for several samples, indicating a concentration below 25 μg mL$^{-1}$.

Concerning the concentrations of infectious KHV, roughly 0.7 log $TCID_{50}$ mL$^{-1}$ of the initial concentration was not recovered in the elution fraction when the SXC was performed with a neutral buffer (Figure 5a). This number was almost 3.0 log $TCID_{50}$ mL$^{-1}$ when loading was performed at pH 6.0. This difference was also detected in the eluate of infectious KHV (Table 1).

The concentration of residual protein and total dsDNA in the eluate fraction was similar for both tested pH values with approximately 2.8–7.5 ng mL$^{-1}$ dsDNA and 54–57 μg mL$^{-1}$ protein.

The maximum loading volumes were determined by the pressure limit of the chromatographic system with a KHV-PEG-feed

of $2 \times 10^6$ TCID$_{50}$ mL$^{-1}$. The lowest loading volume was measured at pH 5.0 (2 mL, $4 \times 10^6$ TCID$_{50}$) and increased by a factor of 1.5–2 in both pH directions. The maximum was reached at pH 7.4 with $4.3 \pm 0.9$ mL ($9 \times 10^6$ TCID$_{50}$), followed by pH 3.0 (approx. 4 mL), and pH 5.0 (approx. 2 mL).

## 3.5 | KHV precipitation, depending on time, PEG concentration and pH

The precipitation kinetics of the clarified KHV cell culture supernatants were analysed depending on the incubation time (0–60 min), the PEG-6000 concentration (0%–12%) and the pH (4–7.4) in CPB. Using the resulting data, a DOE-based model was compiled (Supplementary Material S4.1 and Table S7) and statistically analysed by ANOVA (Supplementary Material S4.1 and Table S8). All three model terms (time, pH and PEG concentration) and their respective interactions were significant ($p \leq .05$) for the precipitate size. Additionally, the factor time (factor C) indicated sedimentation by a quadratic component (C$^2$).

In general, the precipitates increased in size over time (Figure 6). This process was accelerated at high PEG-6000 concentrations and lower tested pH values. The latter two factors affected the system in a reinforcing way, which is exhibited by the size maximum at pH 4 and 12% PEG-6000. Concerning the pH-dependent size without PEG addition, samples at pH 7.4 had an unvaried size distribution over time, with a mean of $129 \pm 18$ nm. At pH 4.0 and 0% PEG, a spontaneous aggregation was observed with mean sizes of up to 1000 nm after 60 min. With the introduction of 12% PEG-6000 on the contrary, the mean diameter of the samples increased four- to 12-fold, with bigger aggregates for lower pH values.

Visualization by bright-field microscopy confirmed an increase in size of the aggregates as predicted by the model (Supplementary Material S4.2 and Figure S6). The structure of those KHV precipitates from the cell culture supernatant, that is KHV, residual cell debris and protein, was of an unordered, random manner.

## 3.6 | Characterization of the KHV

The KHV was characterized concerning its infectivity preservation in the presence of NaCl and its pH-dependent charge (and isoelectric point).

A concentration-dependent KHV inactivation was suggested from the incubation with different NaCl concentrations (Figure 7a). After 2 h incubation time, 1.1 M and 2.1 M NaCl reduced the mean titre significantly by >0.5 log for. Concerning the impact of the storage at −80°C and, thus, one freeze–thaw cycle, no substantial change in the KHV infectivity was observed for any NaCl concentration. Furthermore, no evidence for the reduction in viral DNA was observed, which might be present intra- or extra-viral (data not shown).

For the analysis of the KHV pH-dependent charge, measurements of the zeta potential were undertaken in two different buffer systems, that is PBS supplemented with 0.03% (v/v) polysorbate 20 (PBS-T), and CPB with a pH ranging from 3 to 11. In this range, the isoelectric point, the point of zero charge (0 mV), was located at pH 4 for both buffers (Figure 7b).

## 4 | DISCUSSION

### 4.1 | Evaluating optimal process conditions for a KHV purification by SXC

In this study, the application of the SXC for the purification of (infectious) KHV was evaluated. The study with KHV revealed the highest infectivity yield with 55%, that is a 0.65 log TCID$_{50}$ mL$^{-1}$ loss in the elution fraction, with the highest tested PEG concentration of 12% PEG-6000 at a neutral pH (Figure 5a). In the case of KHV DNA, pH 6 revealed the highest yield in the elution with 34% (Figure 5a). Although the losses were higher at pH 7.4 ($78 \pm 10$%), the concentration of KHV DNA in the elution fraction was increased to $3.9 \pm 2.6 \; 10^9$ cn mL$^{-1}$. It should be mentioned that, under the applied conditions, DNA, which is not related to a complete virus particle, is not targeted by SXC retention with the parameters applied in this study (Levanova & Poranen, 2018). This might explain the higher percentage losses for KHV DNA, which might be present extra-viral in the cell culture supernatant from lysed cells, compared with infectious KHV in the elution. The purity from host cell contaminants of the final KHV eluates was very high with <10 ng mL$^{-1}$ dsDNA and <60 µg mL$^{-1}$ protein. The numbers agree with the results from the literature for Hepatitis C virus (Lothert, Offersgaard, Pihl et al., 2020) and Influenza A virus (Marichal-Gallardo et al., 2017).

Overall, the SXC yield of KHV DNA and of viral infectious particles increased with rising PEG concentrations and molecular weights, with the PEG concentration being the dominant factor (Figures 2 and 3). This was expected as PEG is the driving force of SXC, causing the association of the viral particles and their accretion to the stationary phase (Lee et al., 2012), and was predicted by the offline precipitation kinetics for the KHV cell culture supernatant (Figure 6). Nevertheless, the PEG concentration was shown to be a limiting factor in SXC applications, due to two reasons: on one hand, high viscosities of the PEG solution hinder high flow rates and cause high backpressure (Eilts, Lothert, Orbay et al., 2022); on the contrary, by the formation of large precipitates, filtration effects on the membrane stationary phase induce pore blockages (Eilts, Steger, Lothert, & Wolff, 2022b; Lothert, Sprick, Beyer et al., 2020; Figure 1c). In this study, an interesting effect was observed. Although the maximum loading capacity of the membranes was limited by an increased backpressure (Figure 4), unretained KHV DNA was detected in the flow-through fraction for both tested regenerated cellulose membrane types, 1 and 3–5 µm. This might have originated from extra-viral DNA or
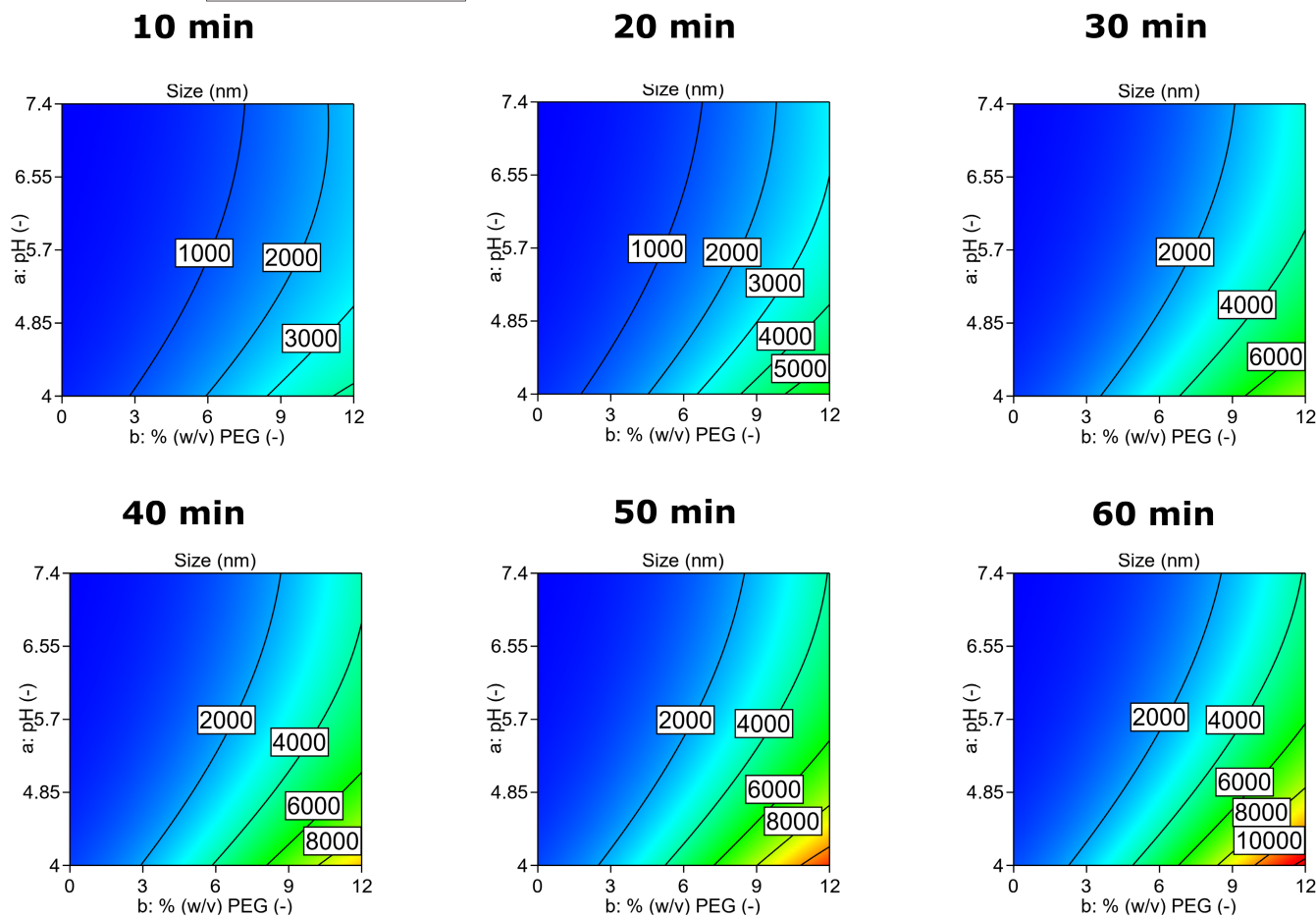
**FIGURE 6** Precipitation kinetics of the KHV with varying pH values and PEG concentrations. Using a design of experiments-based approach, the precipitation kinetics of the KHV were modelled in dependence of the pH (4–7.4) and the PEG-6000 (0–12%) concentration. Thus, a clarified KHV cell culture supernatant was mixed in equal parts with defined buffers, and the samples were analysed using dynamic light scattering. Measurements were conducted on the same sample every 5 min automatically over the course of 60 min. After each incubation step, the sample was visualized by bright-field microscopy in a Neubauer chamber (Figure S5). The kinetic data were statistically analysed (Table S4) and a model of the size response generated. The colouring of the contour plots was coded for the mean sizes as follows: 100–3000 nm (blue), 3000–4000 nm (light blue), 4000–8000 nm (green), 8000–9000 nm (yellow) and 9000–12,000 nm (red).

unretained viral particles. Additionally, the mass balance of KHV in all chromatographic fractions revealed values below 100% for all tested process conditions, which indicated non-eluted KHV on the membranes. This assumption was confirmed by immunoblotting (Supplementary Material S2). A similar observation was reported previously for the Influenza A virus (Marichal-Gallardo, 2019) where the cumulative recovery was above 80%. However, several publications indicated that at optimal process conditions, the maximum loading of the stationary phase with virus particles is not limited by the backpressure, but by the virus breakthrough due to overloading of the stationary phase. This was observed for the 3–5 μm membranes with baculovirus (Lothert, Sprick, Beyer et al., 2020), as well as for the 1 μm membranes with Hepatitis C virus (Lothert, Offersgaard, Pihl et al., 2020), Influenza A virus (Marichal-Gallardo et al., 2017), and Orf virus (Lothert, Pagallies, Feger et al., 2020).

The SXC is, among others, a size-dependent method (Gagnon et al., 2014). Orf virus (140×240 nm) is roughly of similar size to KHV, and the concentration used in the corresponding studies was comparable to the KHV experiments, that is approximately $10^7$ infectious units mL$^{-1}$. However, contrasting with KHV, infectious Orf virus yields were roughly 80% under similar process conditions. Thus, the size of the virus was not decisive for the yield under chosen conditions. Deductively, we hypothesized that the accretion to the stationary phase must additionally be governed by other forces for the KHV than the sole PEG-induced precipitation, for example surface characteristics of the virus. In this study, we could not clarify why the KHV yield increased with increasing PEG concentration, while the total recovery decreased and KHV was still found in the flow-through. Further studies, using highly purified KHV, might help to investigate the binding mechanisms in detail and exclude factors induced by the cell culture broth. Additionally, the implementation of different hydrophilic membrane types, as was done by Lothert, Sprick, Beyer et al. (2020), might be worth investigating to improve KHV retention and elution as well as the binding capacity of the stationary phase.
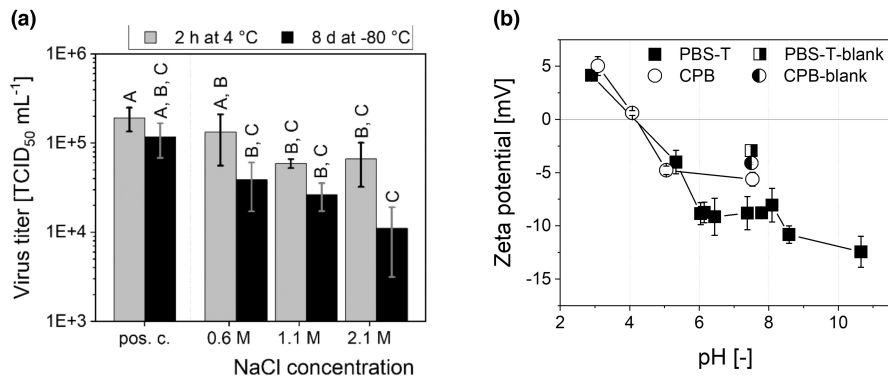
**FIGURE 7** Characterization of the osmotic tolerance of KHV and pH-dependent zeta potential. (a) The osmotic tolerance of infectious KHV was evaluated in the presence of 0.6, 1.1 and 2.1 M NaCl. The positive control (pos. c.) was composed of virus without the addition of salt (0.1 M NaCl originating from medium and PBS). Samples were incubated for 2 h at 4°C (grey), followed by 8 days at −80°C (black). The analysis was conducted with the $TCID_{50}$ assay. A significance test of the data, using an ANOVA with *Tukey* test ($\alpha = 0.05$), was performed. Different letters indicate significant differences. (b) Purified KHV was diluted 1:5 in either a citrate phosphate buffer (CPB) (black squares), pH 3.0–7.5, or in PBS + 0.03% (v/v) polysorbate 20 (PBS-T) (open circles), ranging from pH 3 to pH 11. Immediately after dilution, the zeta potential was measured. The half-filled symbols represent blanks without virus addition. The lines are a guide to the eye. All data shown are mean values with respective standard deviations, $n = 3$.

Nevertheless, insights were gained by the comparison of the cellulose membranes with pore size of 1 and 3–5 μm (Figure 4). The presented study illustrated the increased pressure drop as an answer to pore blockage. As expected, bigger pores caused a reduced backpressure for the same loading volume. Therefore, it can be assumed that pore blockage and fouling take place throughout loading over a longer time period. This was visualized by a decreasing light scattering signal for the 3–5 μm membranes during the loading phase, corresponding with a reduced KHV breakthrough. Supposedly, a gradual accretion to the stationary phase causes reduced pore sizes, whereas the spontaneous contact inducing the association is more likely to happen, and therefore, KHV particles are retained more easily (Lee et al., 2012). To circumvent clogging in the flow-through membranes, tangential flow might be applied. However, this approach reduces the accessible area for binding.

## 4.2 | Precipitation of KHV in the SXC process

As precipitation is the underlying mechanism of SXC, we assumed that the maximum loading capacity can possibly be correlated with the precipitate sizes of a KHV-containing cell culture supernatant. Nevertheless, it should be kept in mind that aggregation itself is not the aspired mechanism of operation of the SXC. It is a limitation, causing the blocking of pores and the increase in backpressures. The recorded kinetics clearly indicated a non-linear increase in aggregate size in the presence of linearly increasing PEG concentrations (Figure 6). Additionally, a reduction in the pH value, which corresponds to an approximation of the isoelectric point of KHV particles (pH 4, Figure 7b), caused a reinforcing mechanism on the precipitate size. This indicated trends for the maximum loading volume in SXC for increased PEG concentrations and for reduced pH values. Similar findings were reported before for Orf virus (Eilts, Lothert,

Orbay et al., 2022) and for latex particles (Eilts, Steger, Lothert & Wolff, 2022b). However, the final precipitate sizes were expected to vary between the static experiments and the dynamic SXC runs. Interestingly, although precipitate sizes in previous experiments with Orf virus were similar to these observed here, the loading capacity of Orf virus was considerably higher throughout the SXC. This supports the hypothesis that the KHV binds to the cellulose membranes by additional mechanisms, which have not been elucidated so far.

Furthermore, we observed a spontaneous aggregation behaviour of the KHV particles in the proximity of pH 4 without the addition of PEG (Figure 6), which corresponded to the isoelectric point of the KHV measured in this study (Figure 7b) and explains rapid pore blockage of the cellulose membranes by spontaneous KHV precipitation (Figure 5a). Additionally, the yield of infectious KHV was reduced at pH values below 7.4. Although the loss of infectivity was expected as the KHV is an enveloped virus, a recent study showed the stability of the virus in the range of pH 5.5–9.5 over the course of 24 h (Amtmann et al., 2020), which is contradictory to the results in this study. Presumably, the higher inactivation rate was caused by the elimination of shielding proteins or other process/medium components throughout the SXC process.

## 4.3 | Limitations of NaCl in the SXC process

In recent publications, SXC was performed with elevated salt concentrations in the elution buffer to increase the yield by reducing unspecific bindings (Lothert, Pagallies, Feger et al., 2020; Lothert, Sprick, Beyer et al., 2020). Although the infectivity of KHV was not reduced considerably in the presence of up to 2.1 M NaCl for average handling periods throughout an SXC run (2 h) or storage at −80°C, a decrease in infectivity with increasing salt concentrations is suggested by the SXC data. The implementation in the SXC process

evidently showed that any elevation of the salt concentration led to a reduced infectivity. Nevertheless, we propose that investigations of other salts following the Hofmeister series can improve the elution of viral particles from the stationary phase, if the infectivity is not affected. The effect of a reduced accretion in the loading phase was reported before for the Orf virus, where kosmotropic salts prevented the retention of Orf virus particles on the stationary phase and, thus, reduced the yield (Eilts, Lothert, Orbay et al., 2022; Lee et al., 2012). We propose that these experiments can be expanded to the elution of virus particles from SXC to dissolve dense precipitates on the stationary phase. This proposal is especially valid considering the positive immunoblots detecting KHV on the cellulose membranes after elution (Supplementary Material S2).

## 4.4 | SXC in relation to other purification methods of KHV

A comparison of the purification success of the KHV itself with the results of previous studies is challenging. To our knowledge, no preparative purification strategies for infectious KHV have been published until now and only a few studies evaluated laboratory-scale purification (Bergmann et al., 2017). The achieved loss of less than 1 log $TCID_{50}$ $mL^{-1}$ in this study is a positive result, considering the sensitivity of infectious KHV (Ullrich et al., 2021), and the set-point for further optimisations. However, several publications purified and concentrated KHV DNA from samples obtained from freshwater to investigate the spread of KHV into the environment (Haramoto et al., 2007, 2009; Honjo et al., 2010; Minamoto et al., 2009; Uchii et al., 2011). A detailed overview is presented in Supplementary Material S5. Here, the recoveries of KHV DNA varied between <1% and 9%. The highest value was reached by Minamoto et al. (2009), applying a filtration cascade, followed by the $Al^{3+}$-cation-coated filter method and a consecutive precipitation. This latter application included the precipitation of KHV with 8% PEG-6000 and 0.4 M NaCl, but no method-specific recoveries were stated (Honjo et al., 2010; Minamoto et al., 2009; Uchii et al., 2011). These concentrations were comparable to the values used in the SXC application; however, it is considered that these experiments targeted DNA, while our work focused on the bigger and less charged KHV particles. Additionally, the pH values applied throughout the primary purification by the authors were not suitable to obtain infectious KHV (Amtmann et al., 2020), and the high salt concentration during precipitation can reduce the viral infectivity (Figure 7a). The latter can be eliminated by the application of the here proposed SXC procedure.

## 5 | CONCLUSION

The purification of viruses used for fish vaccines has been scarcely discussed in the literature, and an application for infectious KHV has not been shown yet. In this work, we presented the first evaluation of the purification of infectious KHV using SXC. The PEG precipitation-related chromatographic method allows for an operation with wide pH and salt ranges. However, throughout processing, the KHV infectivity was reduced at salt concentrations above 0.6 M NaCl and pH values below 7.4. The application of stationary phases with different pore diameters revealed that regenerated cellulose membranes with a nominal pore diameter of 3–5 μm allow for increased loading capacities as compared to 1 μm. The optimal process parameters for the infectious KHV yield were 12% PEG-6000, reaching 55% infectious KHV in the elution fraction, that is a loss of approximately 0.65 log $TCID_{50}$ $mL^{-1}$, at a pH value of 7.4, and 35% KHV DNA at a pH value of 6.0. Until now, few comparable studies on the purification of infectious KHV have been published, and studies on the purification of KHV based on DNA quantification for evaluation reached <10%. Nevertheless, the operability was still impeded by the low maximum loading volumes and the total recoveries of KHV. We assume that it was caused by unanticipated filtration effects. Future research might focus on a modification of loading conditions with reduced PEG concentrations, mixtures of kosmotropic and chaotropic salts as well as tangential or radial flow mode. Additionally, an improvement of the elution with pulsed or gradient salt concentrations could be valuable to investigate. Overall, optimal process parameters between different SXC applications for infectious virus purification vary considerably and the method is still under development to become a platform process.

### CONFLICT OF INTEREST STATEMENT

The authors declare no conflict of interest.

## DATA AVAILABILITY STATEMENT

The data that support the findings of this study are available from the corresponding author, M.W.W., upon request.

## ORCID

*Friederike Eilts* [iD] https://orcid.org/0000-0002-2134-1563

## REFERENCES

Adamek, M., Matras, M., Rebl, A., Stachnik, M., Falco, A., Bauer, J., Miebach, A. C., Teitge, F., Jung-Schroers, V., Abdullah, M., Krebs, T., Schröder, L., Fuchs, W., Reichert, M., & Steinhagen, D. (2022). Don't let it get under your skin! - vaccination protects the skin barrier of common carp from disruption caused by cyprinid herpesvirus 3. *Frontiers in Immunology*, *13*, 787021. https://doi.org/10.3389/fimmu.2022.787021

Alvim, R. G. F., Lima, T. M., Silva, J. L., de Oliveira, P. G. A., & Castilho, L. R. (2021). Process intensification for the production of yellow fever virus-like particles as potential recombinant vaccine antigen. *Biotechnology and Bioengineering*, *118*(9), 3581–3592. https://doi.org/10.1002/bit.27864

Amtmann, A., Ahmed, I., Zahner-Rimmel, P., Mletzko, A., Jordan, L. K., Oberle, M., Wedekind, H., Christian, J., Bergmann, S. M., & Becker, A. M. (2020). Virucidal effects of various agents-including protease-against koi herpesvirus and viral haemorrhagic septicaemia virus. *Journal of Fish Diseases*, *43*, 185–195. https://doi.org/10.1111/jfd.13106

Bergmann, S. M., Jin, Y., Franzke, K., Grunow, B., Wang, Q., & Klafack, S. (2020). Koi herpesvirus (KHV) and KHV disease (KHVD) – a recently updated overview. *Journal of Applied Microbiology*, *129*(1), 98–103. https://doi.org/10.1111/jam.14616

Bergmann, S. M., Lutze, P., Schutze, H., Fischer, U., Dauber, M., Fichtner, D., & Kempter, J. (2010). Goldfish (*Carassius auratus* auratus) is a susceptible species for koi herpesvirus (KHV) but not for KHV disease (KHVD). *Bulletin of the European Association of Fish Pathologists*, *30*(2), 74–84.

Bergmann, S. M., Wang, Q., Zeng, W., Li, Y., Wang, Y., Matras, M., Reichert, M., Fichtner, D., Lenk, M., Morin, T., Olesen, N. J., Skall, H. F., Lee, P. Y., Zheng, S., Monaghan, S., Reiche, S., Fuchs, W., Kotler, M., Way, K., … Kielpinska, J. (2017). Validation of a KHV antibody enzyme-linked immunosorbent assay (ELISA). *Journal of Fish Diseases*, *40*(11), 1511–1527. https://doi.org/10.1111/jfd.12621

Dishon, A., Ashoulin, O., Scott Weber, I. I. I., E., & Kotler, M. (2014). Vaccination against koi herpesvirus disease. In R. Gudding, A. Lillehaug, & Ø. Evensen (Eds.), *Fish vaccination* (Vol. *81*, pp. 321–333). Wiley Blackwell. https://doi.org/10.1002/9781118806913.ch27

Eide, K. E., Miller-Morgan, T., Heidel, J. R., Kent, M. L., Bildfell, R. J., Lapatra, S., Watson, G., & Jin, L. (2011). Investigation of koi herpesvirus latency in koi. *Journal of Virology*, *85*(10), 4954–4962. https://doi.org/10.1128/JVI.01384-10

Eilts, F., Lothert, K., Orbay, S., Pagallies, F., Amann, R., & Wolff, M. W. (2022). A summary of practical considerations for the application of the steric exclusion chromatography for the purification of the Orf viral vector. *Membranes*, *12*(11), 1070. https://doi.org/10.3390/membranes12111070

Eilts, F., Steger, M., Lothert, K., & Wolff, M. W. (2022). The suitability of latex particles to evaluate critical process parameters in steric exclusion chromatography. *Membranes*, *12*(5), 488. https://doi.org/10.3390/membranes12050488

Eilts, F., Steger, M., Pagallies, F., Rziha, H.-J., Hardt, M., Amann, R., & Wolff, M. W. (2022). Comparison of sample preparation techniques for the physicochemical characterization of Orf virus particles. *Journal of Virological Methods*, *310*, 114614. https://doi.org/10.1016/j.jviromet.2022.114614

Gagnon, P., Toh, P., & Lee, J. (2014). High productivity purification of immunoglobulin G monoclonal antibodies on starch-coated magnetic nanoparticles by steric exclusion of polyethylene glycol. *Journal of Chromatography A*, *1324*, 171–180. https://doi.org/10.1016/j.chroma.2013.11.039

Gilad, O., Yun, S., Zagmutt-Vergara, F. J., Leutenegger, C. M., Bercovier, H., & Hedrick, R. P. (2004). Concentrations of a koi herpesvirus (KHV) in tissues of experimentally infected Cyprinus carpio koi as assessed by real-time TaqMan PCR. *Diseases of Aquatic Organisms*, *60*(3), 179–187. https://doi.org/10.3354/dao060179

Gränicher, G., Babakhani, M., Göbel, S., Jordan, I., Marichal-Gallardo, P., Genzel, Y., & Reichl, U. (2021). A high cell density perfusion process for modified vaccinia virus Ankara production: Process integration with inline DNA digestion and cost analysis. *Biotechnology and Bioengineering*, *118*(12), 4720–4734. https://doi.org/10.1002/bit.27937

Haenen, O. L. M., Way, K., Bergmann, S. M., & Ariel, E. (2004). The emergence of koi herpesvirus and its significance to European aquaculture. *Bulletin of the European Association of Fish Pathologists*, *24*(6), 293–307.

Haramoto, E., Kitajima, M., Katayama, H., Ito, T., & Ohgaki, S. (2009). Development of virus concentration methods for detection of koi herpesvirus in water. *Journal of Fish Diseases*, *32*(3), 297–300. https://doi.org/10.1111/j.1365-2761.2008.00977.x

Haramoto, E., Kitajima, M., Katayama, H., & Ohgaki, S. (2007). Detection of koi herpesvirus DNA in river water in Japan. *Journal of Fish Diseases*, *30*(1), 59–61. https://doi.org/10.1111/j.1365-2761.2007.00778.x

Hedrick, R. P., Gilad, O., Yun, S. C., McDowell, T. S., Waltzek, T. S., Kelley, G. O., & Adkison, M. A. (2005). Initial isolation and characterization of a herpes-like virus (KHV) from koi and common carp. *Bulletin of Fisheries Research Agency*, *2*, 1–7.

Honjo, M. N., Minamoto, T., Matsui, K., Uchii, K., Yamanaka, H., Suzuki, A. A., Kohmatsu, Y., Iida, T., & Kawabata, Z. (2010). Quantification of cyprinid herpesvirus 3 in environmental water by using an external standard virus. *Applied and Environmental Microbiology*, *76*(1), 161–168. https://doi.org/10.1128/AEM.02011-09

Hu, F., Li, Y., Wang, Q., Zhu, B., Wu, S., Wang, Y., Zeng, W., Yin, J., Liu, C., Bergmann, S. M., & Shi, C. (2021). Immersion immunization of koi (Cyprinus carpio) against cyprinid herpesvirus 3 (CyHV-3) with carbon nanotube-loaded DNA vaccine. *Aquaculture*, *539*, 736644. https://doi.org/10.1016/j.aquaculture.2021.736644

Jordan, L. K., Amtmann, A., Heidenreich, E., Christian, J., Buchholz, R., & Becker, A. M. (2017). Examination of infection parameters for replication of Israeli isolate of koi herpesvirus in common carp brain cells. *Journal of Virology & Antiviral Research*, *6*(3), 1000176. https://doi.org/10.4172/2324-8955.1000176

Labisch, J. J., Kassar, M., Bollmann, F., Valentic, A., Hubbuch, J., & Pflanz, K. (2022). Steric exclusion chromatography of lentiviral vectors using hydrophilic cellulose membranes. *Journal of Chromatography A*, *1674*, 463148. https://doi.org/10.1016/j.chroma.2022.463148

Lee, J., Gan, H. T., Latiff, S. M. A., Chuah, C., Lee, W. Y., Yang, Y.-S., Loo, B., & Gagnon, P. (2012). Principles and applications of steric exclusion chromatography. *Journal of Chromatography A*, *1270*, 162–170. https://doi.org/10.1016/j.chroma.2012.10.062

Levanova, A., & Poranen, M. M. (2018). Application of steric exclusion chromatography on monoliths for separation and purification of RNA molecules. *Journal of Chromatography A*, *1574*, 50–59. https://doi.org/10.1016/j.chroma.2018.08.063

Liu, L., Gao, S., Luan, W., Zhou, J., & Wang, H. (2018). Generation and functional evaluation of a DNA vaccine co-expressing cyprinid herpesvirus-3 envelope protein and carp Interleukin-1 beta. *Fish & Shellfish Immunology*, *80*, 223–231. https://doi.org/10.1016/j.fsi.2018.05.046

Liu, Z., Wu, J., Ma, Y., Hao, L., Liang, Z., Ma, J., Ke, H., Li, Y., & Cao, J. (2020). Protective immunity against CyHV-3 infection via different prime-boost vaccination regimens using CyHV-3 ORF131-based DNA/protein subunit vaccines in carp Cyprinus carpio var. Jian. *Fish & Shellfish Immunology*, *98*, 342–353. https://doi.org/10.1016/j.fsi.2020.01.034

Lothert, K., Dekevic, G., Loewe, D., Salzig, D., Czermak, P., & Wolff, M. W. (2021). Upstream and downstream processes for viral Nanoplexes as vaccines. In B. A. Pfeifer & A. Hill (Eds.), *Vaccine delivery technology* (Vol. *2183*, pp. 217–248). Springer. https://doi.org/10.1007/978-1-0716-0795-4_12

Lothert, K., Offersgaard, A. F., Pihl, A. F., Mathiesen, C. K., Jensen, T. B., Alzua, G. P., Fahnøe, U., Bukh, J., Gottwein, J. M., & Wolff, M. W. (2020). Development of a downstream process for the production of an inactivated whole hepatitis C virus vaccine. *Scientific Reports*, *10*(1), 3018. https://doi.org/10.1038/s41598-020-72328-5

Lothert, K., Pagallies, F., Eilts, F., Sivanesapillai, A., Hardt, M., Moebus, A., Feger, T., Amann, R., & Wolff, M. W. (2020). A scalable downstream process for the purification of the cell culture-derived Orf virus for human or veterinary applications. *Journal of Biotechnology*, *323*, 221–230. https://doi.org/10.1016/j.jbiotec.2020.08.014

Lothert, K., Pagallies, F., Feger, T., Amann, R., & Wolff, M. W. (2020). Selection of chromatographic methods for the purification of cell culture-derived Orf virus for its application as a vaccine or viral vector. *Journal of Biotechnology*, *323*, 62–72. https://doi.org/10.1016/j.jbiotec.2020.07.023

Lothert, K., Sprick, G., Beyer, F., Lauria, G., Czermak, P., & Wolff, M. W. (2020). Membrane-based steric exclusion chromatography for the purification of a recombinant Baculovirus and its application for cell therapy. *Journal of Virological Methods*, *275*, 113756. https://doi.org/10.1016/j.jviromet.2019.113756

Ma, Y., Liu, Z., Le, H., Wu, J., Qin, B., Liang, Z., Ma, J., Ke, H., Yang, H., Li, Y., & Cao, J. (2020). Oral vaccination using artemia coated with recombinant *Saccharomyces cerevisiae* expressing cyprinid herpesvirus-3 envelope antigen induces protective immunity in common carp (*Cyprinus carpio* var. Jian) larvae. *Research in Veterinary Science*, *130*, 184–192. https://doi.org/10.1016/j.rvsc.2020.03.013

Marichal-Gallardo, P., Börner, K., Pieler, M. M., Sonntag-Buck, V., Obr, M., Bejarano, D., Wolff, M. W., Kräusslich, H. G., Reichl, U., & Grimm, D. (2021). Single-use capture purification of adeno-associated viral gene transfer vectors by membrane-based steric exclusion chromatography. *Human Gene Therapy*, *32*(17–18), 959–974. https://doi.org/10.1089/hum.2019.284

Marichal-Gallardo, P., Pieler, M. M., Wolff, M. W., & Reichl, U. (2017). Steric exclusion chromatography for purification of cell culture-derived influenza a virus using regenerated cellulose membranes and polyethylene glycol. *Journal of Chromatography A*, *1483*, 110–119. https://doi.org/10.1016/j.chroma.2016.12.076

Marichal-Gallardo, P. A. (2019). Chromatographic purification of biological macromolecules by their capture on hydrophilic surfaces with the aid of non-ionic polymers. *Universitäts- Und Landesbibliothek Sachsen-Anhalt*, 1–118. https://doi.org/10.25673/33035

Minamoto, T., Honjo, M. N., & Kawabata, Z. (2009). Seasonal distribution of cyprinid herpesvirus 3 in Lake Biwa, Japan. *Applied and Environmental Microbiology*, *75*(21), 6900–6904. https://doi.org/10.1128/AEM.01411-09

Reed, L. J., & Muench, H. (1938). A simple method of estimating fifty percent endpoints. *American Journal of Epidemiology*, *27*(3), 493–497. https://doi.org/10.1093/oxfordjournals.aje.a118408

Sommerset, I., Krossøy, B., Biering, E., & Frost, P. (2005). Vaccines for fish in aquaculture. *Expert Review of Vaccines*, *4*(1), 89–101. https://doi.org/10.1586/14760584.4.1.89

Uchii, K., Telschow, A., Minamoto, T., Yamanaka, H., Honjo, M. N., Matsui, K., & Kawabata, Z. (2011). Transmission dynamics of an emerging infectious disease in wildlife through host reproductive cycles. *The ISME Journal*, *5*(2), 244–251. https://doi.org/10.1038/ismej.2010.123

Ullrich, J., Christian, J., Bergmann, S. M., Oberle, M., & Becker, A. M. (2021). Stability of viral haemorrhagic septicaemia virus, infectious hematopoietic necrosis virus and cyprinid herpesvirus 3 in various water samples. *Journal of Fish Diseases*, *44*(4), 379–390. https://doi.org/10.1111/jfd.13321

Vandenberg, G. W. (2004). Oral vaccines for finfish: Academic theory or commercial reality? *Animal Health Research Reviews*, *5*(2), 301–304. https://doi.org/10.1079/AHR200488

Wang, Y., Zeng, W., Li, Y., Liang, H., Liu, C., Pan, H., Lee, P., Wu, S., Bergmann, S. M., & Wang, Q. (2015). Development and characterization of a cell line from the snout of koi (*Cyprinus carpio* L.) for detection of koi herpesvirus. *Aquaculture*, *435*, 310–317. https://doi.org/10.1016/j.aquaculture.2014.10.006

Yanong, R. P., & Erlacher-Reid, C. (2012). *Biosecurity in aquaculture: Part 1: An overview*. USDA Southern Regional Aquaculture Center.

## SUPPORTING INFORMATION

Additional supporting information can be found online in the Supporting Information section at the end of this article.